BULLETIN OF THE POLISH ACADEMY OF SCIENCES
TECHNICAL SCIENCES, Vol. 68, No. 3, 2020
DOI: 10.24425/bpasts.2020.133380

Experimental investigation and characteristics of multiwalled carbon nanotube aqua nanofluids from a flat plate heater surface in a pool

D. VASUDEVAN[1]*, D. SENTHIL KUMAR[2], A. MURUGESAN[1], and C. VIJAYAKUMAR[3]

[1] Department of Mechanical Engineering, K S Rangasamy College of Technology, Tiruchengode 637 215, India
[2] Department of Mechanical Engineering, Sona College of Technology, Salem 636 011, India
[3] Department of Mechatronics Engineering, K S Rangasamy College of Technology, Tiruchengode 637 215, India

Abstract. In this experimental investigation, the critical heat flux (CHF) of aqua-based multiwalled carbon nanotube (MWCNT) nanofluids at three different volumetric concentrations 0.2%, 0.6%, and 0.8% were prepared, and the test results were compared with deionized water. Different characterization techniques, including X-ray diffraction, scanning electron microscopy and Fourier transform infrared, were used to estimate the size, surface morphology, agglomeration size and chemical nature of MWCNT. The thermal conductivity and viscosity of the MWCNT at three different volumetric concentrations was measured at a different temperature, and results were compared with deionized water. Although, MWCNT-deionized water nanofluid showed superior performance in heat transfer coefficient as compared to the base fluid. However, the results proved that the critical heat flux is increased with an increase in concentrations of nanofluids.

Key words: nanofluids, critical heat flux, heat transfer coefficient, boiling, heat transfer enhancement.

1. Introduction

Boiling is a very efficient mode to transfer heat at a given temperature because of the large latent heat of vaporization. The term boiling will be classified into two categories: flow and pool. The flow of fluid move along hot surfaces is defined as flow boiling, while the fluid boiling in a stationary hot pool is called pool boiling. In this paper, the liquid above the hot surface is essentially stagnant and in contact with a hot solid surface. Nukiyama et al. have done the first experimentation of boiling heat transfer mechanism in 1934 [1–2]. Pool boiling is effective in heat transfer since latent heat of evaporation takes place, which increases the heat flux. Hence, boiling heat transfer is important in the field of thermal systems, and it is exclusively used in power plants [3], high-powered electronic devices [4], heating, ventilation and air conditioning (HVAC) systems [5], nuclear reactors [6–7], automotive industry [8], and solar collectors [9]. The wider application shows the importance of the heat transfer enhancement study in pool boiling. Experimental studies investigating the pool boiling phenomena were carried out by many researchers. Further, numerical studies have been done by many researchers to predict the actual CHF [10–11] and theoretical model [12–13].

During the past decades, CHF enhancement in pool boiling by changing fluid thermo-physical properties has drawn great attention. A comprehensive review reported on the effect of nanofluid in the pool boiling heat transfer enhancement and concluded that nanofluid research is not sufficient [14]. Further, the authors concluded that the nanofluids have good thermo-physical properties compared to convention fluids. Dispersion of cylindrically shapes nanoparticles like CNT exhibited high viscosity enhancement compared to spherically shaped nanoparticles [15]. The nanofluids were obtained by the dispersion of ultrafine nanoparticles with conventional fluids such as water, ethylene glycol, etc., and the nanoparticle ranges differed from 1 to 100 nm. Preparations of nanofluids had been reviewed and highlighted the method of preparation [16]. Different type of nanoparticles like CuO [17], MWCNT [18], SiO_2 [19], TiO_2 [20], Graphene oxide [21], ZrO_2 [22] and Al_2O_3 [23] with this wide range, various concentrations had been examined to enhance the CHF value. Based on the above literature, it can be concluded that multiwalled carbon nanotubes are suitable for heat transfer enhancement applications with their distinct characteristics such as higher stability, lower corrosion and higher thermal conductivity. Also, the deposition of such nanoparticles on the heater surface tends to enhance the CHF in pool boiling. To the best of our knowledge, no such experimental investigations were done earlier to study effect of CHF on copper plate heater with MWCNT nanofluids. Hence, this present work aims to enhance the CHF of base fluid by adding MWCNT nanofluids.

2. Experimentation or methodology

In this section, thermophysical properties of nanofluid and characterization techniques have been used to identify the mechanism behind the CHF enchancement. Secondly, an experimental investigation had been carried out with different volume concentration of nanofluids over a copper plate heater.

*e-mail: vasudevan.vi@gmail.com

Manuscript submitted 2019-10-05, revised 2019-12-18, initially accepted for publication 2020-02-20, published in June 2020

2.1. Preparation of nanofluid. Preparation of nanofluids is the first key step during experimental studies with nanofluids. Some unique necessities are essential e.g. even and steady suspension, strong suspension, negligible agglomeration of particles, no chemical change in the fluid, etc. Nanofluids are produced by dispersing nanometer scale solid particles into the base liquids such as water, ethylene glycol (EG), oils, etc. Two kinds of methods have been employed in producing nanofluids. One is a single-step method and the other is a two-step method. In this study, the nanofluid has been prepared by the two-step method. First, the MWCNT is weighed by the use of a precision balance. It is then dispersed with a known quantity of DI water to obtain 0.2%, 0.6% and 0.8% concentrations of MWCNT based nanofluids. Figure 1 shows the MWCNT nanoparticle with deionized water at different concentrations, such as 0.2%, 0.6% and 0.8%. The nanofluids are prepared by mixing the powder particles in deionized water without delay in various steps; however, no surfactant is used in this work. To obtain homogenous and stable suspension, the prepared nanofluids have been kept in ultrasonic vibrator for 12 h. Stability test were performed after preparing the nanofluid. The fluid was kept idle for 30 days and changes in the physical appearance have been monitored. Figure 1 has been taken on 30th day after, and it was noticed that there are no changes in the physical appearance. The prepared nanofluids are used for the experimental study.

Fig. 1. MWCNT nanofluids at various concentrations

3. Characterizations of MWCNT/ water nanofluid

3.1. X-ray diffraction (XRD) spectra of MWCNT. The XRD spectra shown in Fig. 2 are used to estimate the purity, crystal size and degree of oxidation of MWCNT. The most

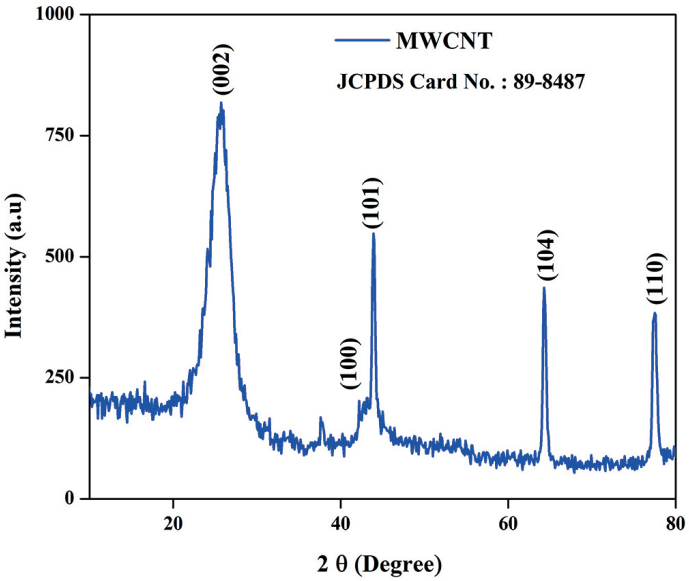

Fig. 2. XRD pattern of MWCNT

elevated peak noticed at $2\theta = 26.3°$ is assumed to be the characteristic peak of MWCNT while the three low intensity peaks at $2\theta = 42.1°$, 44.5°, 64.3° and 77.51° attributes to the diffraction signature of the distance between the walls of CNTs and the interwall spacing respectively for (100) (101) (104) and (110) planes. It is evident that the prepared powder sample contains pure form of MWCNT through the similarity observed between the XRD profile of prepared sample and pure MWCNT acquired through JCPDS card No.: 89–8487. The diffraction peak noticed around 26° validates the existence of hexagonal structure (P63mc space group) in the MWCNT.

3.2. SEM and EDAX image of MWCNT. SEM image is used to measure the surface morphology of nano-powder. MWCNT were received from M/s Platonic Nanotech Private limited (India). The physical properties of MWCNT are listed in Table 1 and the morphological characterization for MWCNT was obtained by using scanning electron microscopy as shown in Fig. 3 and it is evident that MWCNT exists in the form of wrinkled thread-like structure with curled surface morphology. Secondly, some irregularities and porous zone noticed on the MWCNT surface can be attributed to difference in thermal

Table 1
Physical properties of MWCNT nanoparticles

Chemical symbol	C
Appearance	Black
Purity	97%
Diameter	5-20 nm
Specific Surface Area	90–350 m^2/g
Density	3.250 g/cm^3

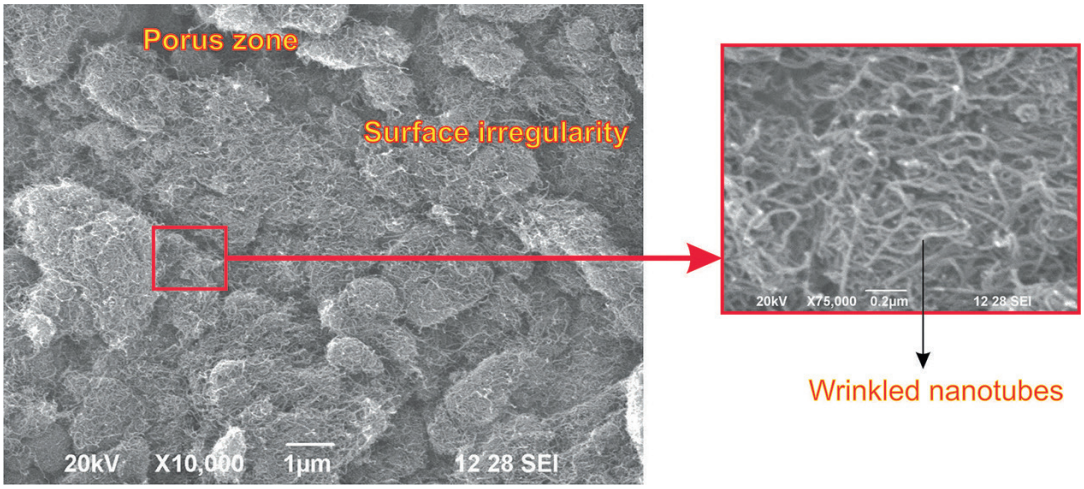

Fig. 3. SEM image of MWCNT

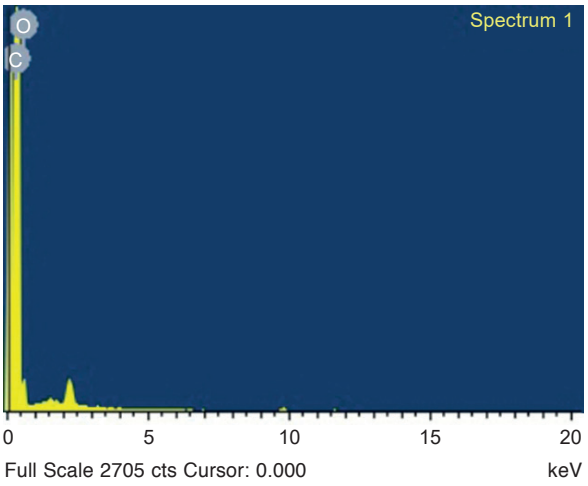

Fig. 4. EDAX image of MWCNT

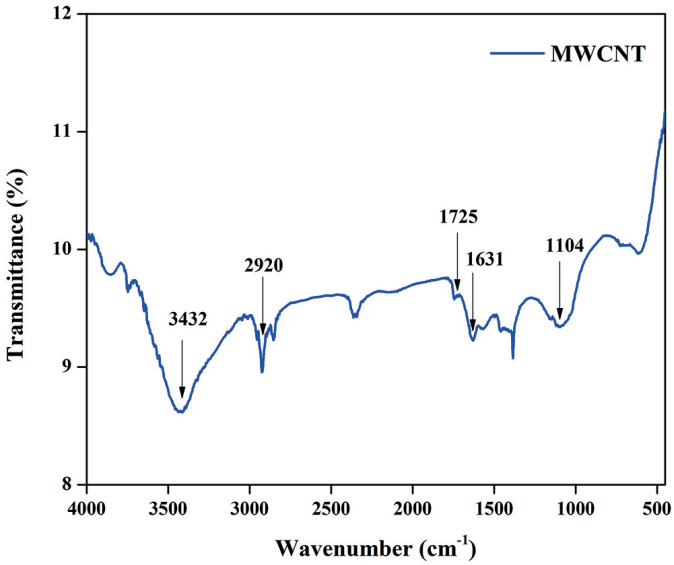

Fig 5. FTIR spectrum of MWCNT

conductivity [24]. Figure 4 depicts the elemental analysis of MWCNT and it presents no other elements except carbon and oxygen. It validates that MWCNT used in this investigation as high in purity and in association with XRD results.

3.3. FT-IR spectra of MWCNT. FTIR is considered an appropriate tool to identify the presence of functional groups attached to the MWCNTs. The FTIR spectrum of MWCNT shown in Fig. 5 depicts a vulnerable peak attributed to the carbonyl stretch of carboxylic acid group at 1725 cm^{-1}. Accordingly, the peaks noticed around 3432 cm^{-1} and 1631 cm^{-1} represents the characteristic of the stretching vibrations and bending of O–H bonds respectively. This can be due to the presence of residual water in the sample or it can be attributed to the oscillation of carboxyl groups adsorbed on the external walls of MWCNTs from environment. A small peak located around 1104 cm^{-1} represents C–O stretching groups and the peak located at 2920 cm^{-1} corresponds to C–H bond within the MWCNT [25].

4. Thermo-physical properties of MWCNT nanofluids

It is necessary to find the transport properties of nanofluid to study the heat transfer phenomena. The heat transfer performance of the nanofluids depends on the thermal conductivity, viscosity, specific heat and density of the nanofluids. In general, the properties of MWCNT nanofluid depend upon physical properties, and they can be determined using analytical methods. The involvement of surface molecules in the heat transfer process, which depends upon the size and shape of the particles, and the flow phenomenon of a liquid-solid solution which depends on the hydrodynamic force acting on the surface of solid particles. The following equation has been used to compute the exact volume of nanoparticles:

$$\Phi_v = \frac{1}{\left(\frac{1-\Phi_m}{\Phi_m}\right)\frac{\rho_p}{\rho_f}+1} \tag{1}$$

From the following (1) the density of nanofluid is derived, and the relation for heat capacity of nanofluids were driven [26]

$$\rho = \rho_f(1-\Phi_v) + \rho_p\Phi_v \tag{2}$$

$$\rho C_p = \rho_f C_{pf}(1-\Phi_v) + \rho_p C_{pp}\Phi_v \tag{3}$$

$$\frac{k}{k_f} \approx 1 + n\Phi_v \tag{4}$$

where $n = 3/\psi$, and ψ is the sphericity of nano particles, it is defined as the ratio of surface area of a sphere with a volume equal to that of the surface area of a test particle were sphericity of sphere is 1.0 and other nanoparticles, it varies from 0.5 to 1.0. The thermal conductiviy of the fluids depends on particle volume fraction and sphericity as well. This finding demonstrates the feasibility of MWCNT nanofluids having the ability of increasing the thermal conductivity of conventional heat transfer fluids. Brinkman [27] the following can be used for the prediction of viscosity of nanofluid.

$$\mu = \mu_f(1 + 0.25\Phi_v) \tag{5}$$

From the above equations, the major properties of MWCNT nanofluids for various concentrations were calculated and given in Table 2.

Table 2
Thermo-physical properties of MWCNT nanoparticles

MWCNT nanofluid	1	2	3
Φ_m (%)	0.1310	0.2832	0.4116
Φ_v (%)	0.2000	0.6000	0.8000
ρ/ρ_o	0.9982	0.9971	0.9932
C_p/C_{po}	0.9984	0.9973	0.9937
k/k_o	1.0350	1.0180	1.0080
μ/μ_o	1.0030	1.0061	1.0120

5. Experimental setup and procedure for boiling heat studies

The schematic representation of a flat plate heater experimental set up facility is illustrated in Fig. 6. It consists of a borosilicate vessel, pressure plate, preheater, condenser, and DC electricity supply. The borosilicate glass vessel is of internal diameter 60 mm and thickness of 4 mm.

This experimental setup, which consisted of polished square copper test heater surface of 40 mm and 0.4 mm thickness, and the test section two was brazed with a copper bus bar of 190 mm and length 30×5 mm cross-section. This heater is tightly attached to the slot which was made in the teflon sleeve

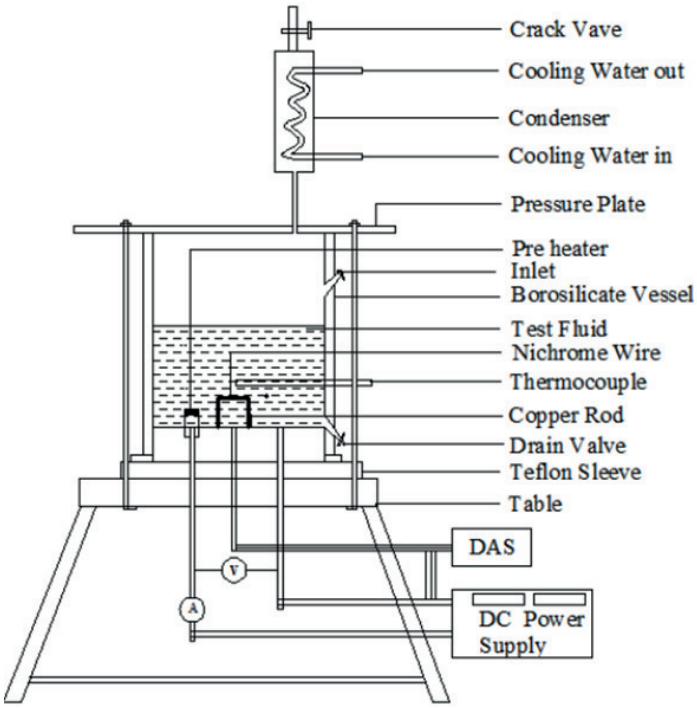

Fig. 6. Experimental setup to investigate the pool boiling heat transfer

of diameter 60 mm via the silicon disc and the power supply is connected to the other end of the copper bar.

The unit of a step-down transformer which has the variable capacity of 10 kVA, and it is controlled using dimmer stat. To measure the temperature of the test surface area, 5 T-Type thermocouples are used, fitted in five different positions. The fitted thermocouple leads and voltage are taken out via capillary holes made in a Teflon sleeve and it is connected to the data acquisition system.

The borosilicate vessel has the provision with the inlet, cleaning vent, drain valve and one reflux glass condenser as shown in Fig. 6. The mild steel of 6 mm diameter rod is used to arrest the immovable of the vessel; one end is connected with base and another end with pressure plate under this silicon rubber proof for preventing the lead. Prior to experiments, the borosilicate vessel and test section are thoroughly cleaned with DI water, then cleaned with cleaning soap water, and then subsequently cleaned with acetone to remove the scales and dirt. After cleaning, the test section is filled with DI water which is stabilized by heating for 12 h at a heat flux of 500 kW/m^2, afterwards; the test section is allowed to cool for another 12 h.

In the initial stage of data acquisition device with the lowest heat flux of 50 kW/m^2 is used to maintained the saturation temperature of the test fluid, and generated steam is passed via the condenser to remove the dissolved gases which existing in the test vessel. Simultaneously, cooling water is passed through the reflux condenser by means of vapor generated by boiling of water, which is condensed and drained again to the pool due to the presence of gravity of the test fluid. Then test heater heat flux is step by step increased from the range 50 kW/m^2 to just below the burnout level and data to be acquired in each

step. After the experiments, the deionized water is replaced by deionized – MWCNT nanofluids of the concentrations of 0.2%, 0.6%, and 0.8% by volume. After each test is conducted, the vessel is checked and the heater is cleaned with soap water, having to maintain the entire test under atmospheric pressure.

6. Data reduction

The wall temperature (T_w) of plate heater test-section is determined with plate thickness (δ), thermal conductivity (kW) and internal volumetric heat generation (q_g) from (6):

$$T_w = \frac{\dot{q}_g}{2k_w}\delta^2 + T_b \tag{6}$$

where T_b is the average bottom surface temperature of test heater and it is determined from the following equation:

$$T_b = \frac{T_1 + T_2 + T_3 + T_4 + T_5}{5} \tag{7}$$

where T_1, T_2, T_3, T_4 and T_5 are the bottom surface temperature of the test heater positioned at different places. The average heat transfer coefficient evaluated from the following equation:

$$h = \frac{q}{T_w - T_{sat}} \tag{8}$$

All the precautions have been taken to limit the errors in the experimentation, yet some errors have probably appeared. The uncertainty analysis of the instrument in the calculation yields 0.42% for heat flux, 0.75% for outer wall diameter, 0.19% for inner wall diameter, 0.39% for heat energy supplied to the test surface, and 4.32% for average heat transfer coefficient.

7. Results and discussion

In order to make sure of the integrity of the experimental setup, the data from the boiling of deionized water over a flat plate test heater have been analyzed. To determine the pool boiling characteristics of nanofluids these data shall also be used as reference data.

The predicted Cornwell–Houston correlation [27] given by (9) and (10) have been compared with the heat transfer coefficient for the pool boiling of deionized water.

$$Nu = 9.7P_c^{0.5}F_p\,\mathrm{Re}^{0.67}\,\mathrm{Pr}^{0.4} \tag{9}$$

$$F_p = 1.8P_r^{0.17} + 4P_r^{1.2} + 10P_r^{10} \tag{10}$$

Figure 7 presents the comparison of experimental result with Cornwell-Houston correlation [28], taking heat transfer coefficient, h as ordinate for the pool boiling of water over the flat plate heater surface and heat flux, q, as abscissa. The experimental results for the pool boiling of deionized water

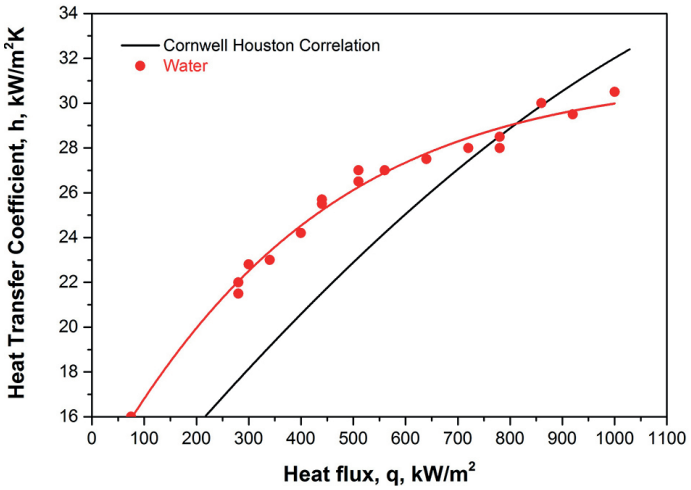

Fig. 7. Comparison of experimental data with Cornwell Houston correlation

over a flat plate test heater are found to be in good conformity with those predicted by Cornwell–Houston [28] correlation. Figure 7 also shows that the low heat flux of 200 kW/m^2 Cornwell–Houston correlation underestimates the experimental values by 40%, the predictions from correlation are convergent to the experimental values when heat flux increases. The heat transfer performance of the test surface shows better results in association with higher bubble generation frequency and higher bubble nucleation [29]. Hence, high bubble dynamic due to the higher heat flux at heat transfer curve for experimental data converges towards the predicted values. Figure 8 shows the relation between wall superheat and heat flux. It is observed that the boiling curve for deionized water-MWCNT nanofluid shift towards right indicates for a given heat flux of the wall a superheat decrease with increase in concentration, and heat transfer increases with increase in the concentration of MWCNT. A potential reason for this shift may be the filling

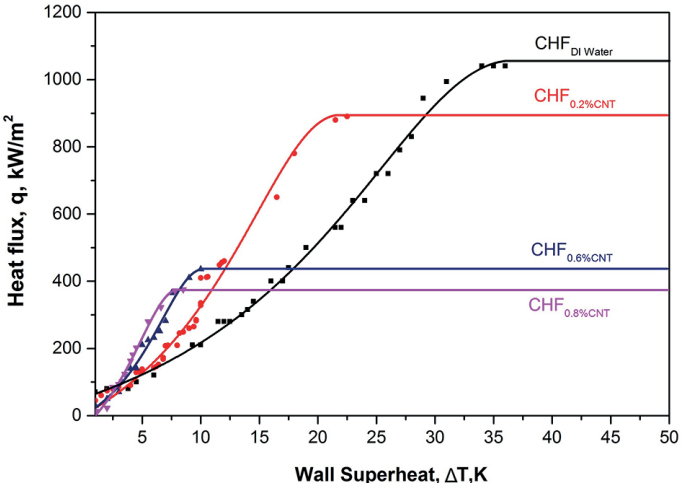

Fig. 8. Comparison of boiling curves of MWCNT nanofluids with deionized water (ΔT Vs q)

up of surface cavities by nanoparticles and, as a result, reducing the number of nucleation sites on the test-section surface. Therefore, concentrations of MWWCNT increases with the heat transfer coefficient are increased. It is also observed that the increase in MWCNT concentrations with the CHF of nanofluids decreases. This clearly indicates that the increase of nanoparticles concentration with the boiling heat transfer decreases, due to alteration in the topography and microstructure of the test-section by the deposition of nanoparticles.

At the same time, as shown in Fig. 9, the nanofluid containing 0.2% by volume of MWCNT in deionized water, the heat transfer coefficient increases first, for the given low heat fluxes up to 75 kW/m^2 and then it decreases with the increase in heat flux. This phenomenon may stem from the fact that the heat fluxes with the bubble generation are very low. The MWCNT penetrates the bubbles which are formed near the test-section surface and phenomenon of smaller size bubbles by splitting larger size bubbles. Hence, resulting in the increase in heat transfer at lower heat fluxes by generation of large number of small bubbles. When heat flux increases, more bubbles are generated on the test section and the probability of bubble penetration and contact of thermal boundary layer by MWCNT becomes bleak. From this study, it is concluded that MWCNT enhances boiling heat transfer significantly at lower heat fluxes and lower concentrations with base fluid and the concentration increases; the heat transfer coefficient also increases, due to increasing surface area of MWCNT.

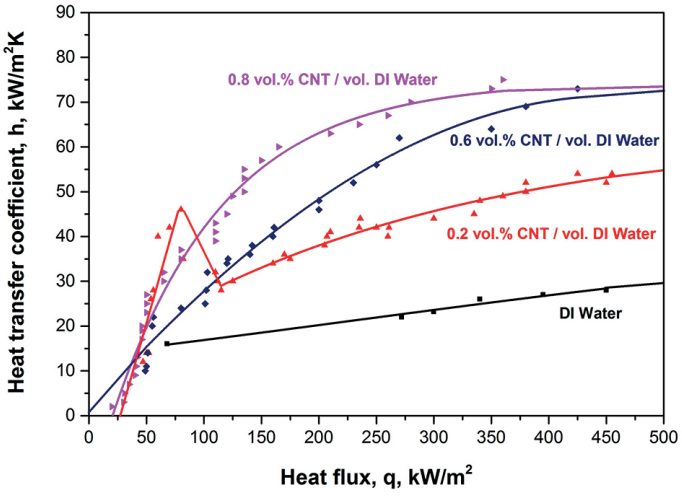

Fig. 9. Boiling curves of MWCNT-nanofluids with deionized water (h Vs q)

For 500 kW/m^2 heat flux, the heat transfer coefficient is enhanced by 2.3, 3.2 and 4 times for 0.2%, 0.6% and 0.8% volume concentration of MWCNT, respectively, as shown in Fig. 10. The physical phenomenon might also be due to bubble generation being very low at lower heat fluxes, due to the higher thermal conductivity of MWCNT penetrating the bubbles which formed near the test section surface (thermal boundary layer); the phenomenon causes splitting of larger size bubbles by

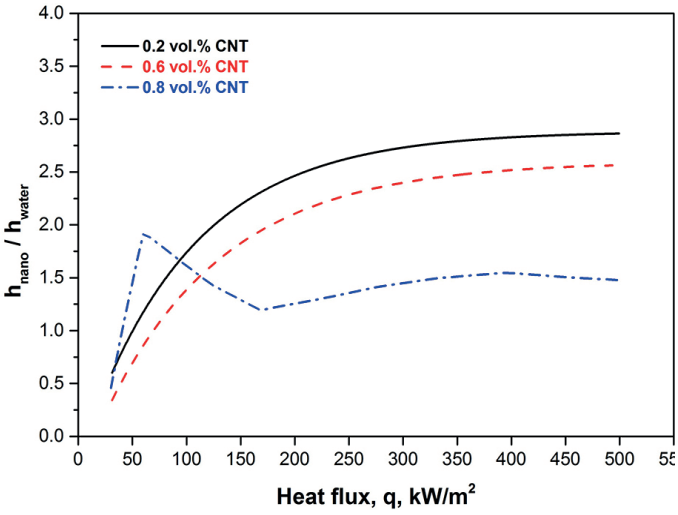

Fig. 10. Heat transfer coefficient enchancement (h Vs q)

smaller size bubbles. Hence, a large number of small bubbles are generated, ensuing in the increase in heat transfer at lower heat fluxes. As the heat flux increases, more bubbles are generated and the possibility of bubble penetration and contact of the thermal boundary layer through MWCNT becomes bleak. From this observation, it is concluded that MWCNT enhances the heat transfer rate at lower heat fluxes and lower concentrations with base fluids. When the concentration increases with increases in heat transfer coefficient due to the increase in surface area of MWCNT.

The thermal conductivity of the working fluid is enhanced due to the high region, providing heat transfer by using conduction at low resistance. The heat transfer rate will increase due to the significance effect of higher thermal conductivity and larger specific region. At the same time, as represented in Fig. 9, in 0.2% MWCNT nanofluids remaining in deionized water, the HTC increases the heat fluxes up to 81 kW/m^2 and then decreases with gradual increasing order of the heat flux.

The HTC is enhanced by 1.4, 2.5 and 3.2 times the HTC of deionized water for 0.2%, 0.6%, and 0.8% volume concentrations of MWCNT in deionized water, respectively, for the given heat flux of 500 kW/m^2, as observed from Fig. 10. The bubble generation is very low at lower heat fluxes and higher thermal conductivity of MWCNT infiltrates into the bubbles that form near the test surface (thermal boundary layer), the phenomenon results in the splitting of bigger size bubbles into smaller bubbles. Hence, a high number of tiny bubbles are produced, ensuing in increase in heat transfer at lower heat fluxes. When the heat flux increases, the bubble generation and penetration result in the thermal boundary layer with MWCNT nanofluids becoming bleak. From this investigative experiment, it is concluded that MWCNT enhances the heat transfer rate even at lower heat fluxes and lesser concentrations of nanoparticles in base fluids.

The concentration of MWCNT increases with CHF increase as shown in Fig. 11. The increase in CHF reaches its maximum at 1.0% concentration.

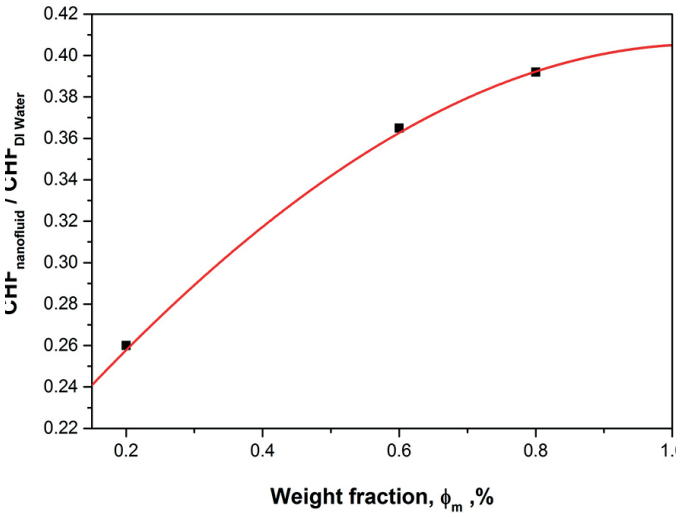

Fig. 11. CHF increase with concentration of MWCNT nanofluid

7.1. Surface wettability behavior and roughness of MWCNT/water nanofluids on heating surfaces. A liquid's capability to interact with solid surface denotes its wettability and it mainly depends on the contact angle. It plays a major role in the heat transfer applications and hence, this study is extended to investigate the boiling heat transfer rate of the MWCNT/deionized water nanofluids by measuring contact angle against copper sheet. The increases in surface roughness of the MWCNT increase the contact area with working fluid, thereby improving its wettability; this factor could result in the CHF enhancement of the nanofluid [24]. In particular, the contact angle of the developed nanofluid increases with roughness and concentration, and so the CHF value becomes elevated at higher concentrations. [30–31]. The contact angle was measured by using dynamic contact angle and tensiometer (Model: DCAT IIEC, Data physics instruments GmbH, Germany), while nano indentation method was adopted to estimate surface roughness. The contact angle of the nanofluid increases with concentration i.e., 98° (0.2%) to 130° (0.8%); also, the average roughness elevates from 41 nm (0.2%) to 110 nm (0.8%), as shown in Fig. 12. The results acquired in this investigation correlate with the statement "an increase in BHT with rough surface is due to the increased surface roughness value" reported by Harish et al. [32]. The surface morphology, namely wettability and surface tension, is the reason for departure of bubbles on the test section. The phenomenon of increase in CHF is not only due to the increase in concentration, but also due to the modified surface [30–32].

8. Conclusion

The experimental investigation was carried out and the following conclusions were drawn:

- the dispersion of MWCNT nanofluids in deionized water reveals significant CHF enhancement in pool boiling experiments with flat plate heater;
- the experimental results proved that MWCNT nanofluids show superior performance in heat transfer coefficients when compared to base fluid;
- it can be predicted that HTC decreases with increase in nanoparticle concentration using Nusselt. The heat transfer rate is enhanced by 7.2% and HTC by 18% for MWCNT nanofluid when compared with deionized water;
- CHF increases with the deposition of MWCNT owing to the alteration in topology and microstructure;
- wettability on the rough surface increases the heat transfer rate;
- CHF enhancement is higher in rough surface when compared with smooth and polished surface due to wettability.

Hence the authors have stated that MWCNT nanofluid is a suitable fluid for thermal systems with effective heat transfer rates.

Acknowledgments. The authors are grateful to acknowledge the support provided by DST-FIST (SR/FST/College-235/2014 dated 21.11.2014) and DBT-STAR (BT/HRD/11/09/2018 dated 27.02.2018), Government of India for carrying out this research work.

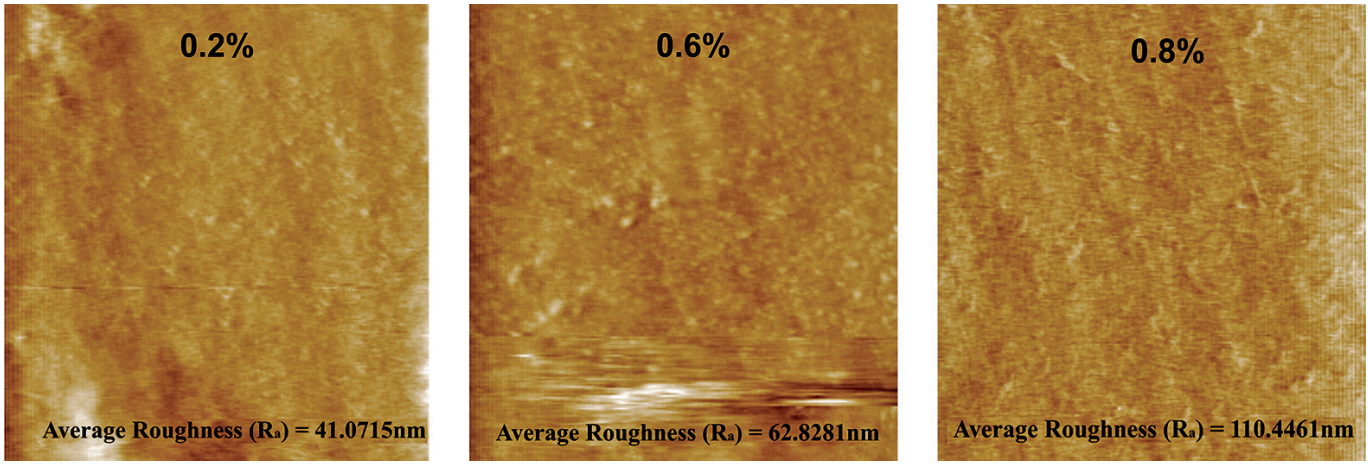

Fig. 12. Nano indentation image of rough surface after boiling with MWCNT-deionized water nanofluids

References

[1] S. Nukiyama, "Maximum and Minimum values of heat transmitted from metal to boiling water under atmospheric pressure", *Soc. Mech. Engng.* 37, p. 206, (1934).

[2] S. Nukiyama, "The maximum and minimum values of the heat Q transmitted from metal to boiling water under atmospheric pressure", *Int. J. Heat Mass Transf.* 9(12), 1419–1433, (1966).

[3] H. Babar, M. U. Sajid, and H. M. Ali, "Performance improvement of the heat recovery unit with sequential type heat pipes using Tio_2 nanofluid", *Thermal science*, pp. 303–303 (2017).

[4] A. M. Siddiqui, "Evaluation of Nanofluids Performance for Simulated Microprocessor", *Therm. Sci.* 21(5), 2227–2236 (2017).

[5] E.Firouzfar, "Energy saving in HVAC systems using nanofluid", *Appl. Therm. Eng.* 31(8), 1543–1545 (2011).

[6] J.Buongiorno, "Nanofluids for enhanced economics and safety of nuclear reactors: an evaluation of the potential features, issues, and research gaps", *Nucl. Technol.* 162(1), 80–91 (2008).

[7] I.C. Bang and J.H. Kim, "Thermal-fluid characterizations of ZnO and SiC nanofluids for advanced nuclear power plants", *Nucl. Technol.* 70(1), 16–27, (2010).

[8] H.M. Ali, "Heat transfer enhancement of car radiator using aqua based magnesium oxide nanofluids", *Therm. Sci.* 19(6), 2039–2048 (2015).

[9] M. Rahman, "Effect of solid volume fraction and tilt angle in a quarter circular solar thermal collectors filled with CNT–water nanofluid", *Int. Commun. Heat Mass Transf.* 57, 79–90 (2014).

[10] S.J. Kim, I.C. Bang, J. Buongiorno, and L.W. Hu, "Study of pool boiling and critical heat flux enhancement in nanofluids", *Bull. Pol. Ac.: Tech.* 55(2), 211–216, (2007).

[11] J.T. Cieśliński, and T.Z. Kaczmarczyk "Pool boiling of nanofluids on rough and porous coated tubes: experimental and correlation", *Bull. Pol. Ac.: Tech.* 35(2), 3–20 (2014)

[12] H. Zhao and A. Williams, "Predicting the critical heat flux in pool boiling based on hydrodynamic instability induced irreversible hot spots", *Int. J. Multiph. Flow* 104, 174–187 (2018).

[13] J. Wang, M. Diao, and X. Liu, "Numerical simulation of pool boiling with special heated surfaces", *Int. J. Heat Mass Transf.* 130, 460–468 (2019).

[14] A. Khan and H. Muhammad Ali, "A Comprehensive review on pool boiling heat transfer using nanofluids", *Therm. Sci.* OnLine-First Issue 00, 72–72 (2019).

[15] H. Babar, M. Usman Sajid, and H. Muhammad Ali, "Viscosity of hybrid nanofluids: A critical review", *Therm. Sci.* OnLine-First Issue 00, 15–15 (2019).

[16] V. Fuskele and R.M. Sarviya, "Recent developments in Nanoparticles Synthesis, Preparation and Stability of Nanofluids", *Mater. Today Proc*. 4(2), 4049–4060 (2017).

[17] A.R. Yagnem and V. S., "Heat transfer enhancement studies in pool boiling using hybrid nanofluids", *Thermochim. Acta* 672, 93–100 (2019).

[18] M. Xing, J. Yu, and R. Wang, "Effects of surface modification on the pool boiling heat transfer of MWNTs/water nanofluids", *Int. J. Heat Mass Transf.* 103, 914–919 (2016).

[19] Y. Hu, Z. Liu, and Y. He, "Effects of SiO_2 nanoparticles on pool boiling heat transfer characteristics of water based nanofluids in a cylindrical vessel", *Powder Technol*. 327, 79–88 (2018).

[20] S. Mori, F. Yokomatsu, and Y. Utaka, "Enhancement of critical heat flux using spherical porous bodies in saturated pool boiling of nanofluid", *Appl. Therm. Eng.* 144, 219–230, (2018).

[21] S.D. Park et al., "Effects of nanofluids containing graphene/graphene-oxide nanosheets on critical heat flux", *Appl. Phys. Lett.* 97(2), 023103 (2010).

[22] S.J. Kim, I.C. Bang, J. Buongiorno, and L.W. Hu, "Effects of nanoparticle deposition on surface wettability influencing boiling heat transfer in nanofluids", *Appl. Phys. Lett.* 89(15), 153107 (2006).

[23] L.L. Manetti, M.T. Stephen, P.A. Beck, and E.M. Cardoso, "Evaluation of the heat transfer enhancement during pool boiling using low concentrations of Al_2O_3-water based nanofluid", Exp. *Therm. Fluid Sci.* 87, 191–200, (2017).

[24] R. Kamatchi and S. Venkatachalapathy, "Parametric study of pool boiling heat transfer with nanofluids for the enhancement of critical heat flux: a review", *Int. J. Therm. Sci*. 87, 228–240 (2015)

[25] H. Kitamura, M. Sekido, H. Takeuchi, and M. Ohno, "The method for surface functionalization of single-walled carbon nanotubes with fuming nitric acid", *Carbon* 49, 3851–3856, (2011).

[26] Y. and Li, "Heat transfer enhancement of nano fluids", *Int. J. Heat Fluid Flow* 21, 58–64 (2000).

[27] H.C. Brinkman, "The viscosity of concentrated suspensions and solutions", *J.Chem. Phys*. 20, 571–581(1952).

[28] K. Cornwell, S, and D. Houston, "Nucleate pool boiling on horizontal tubes: a convection-based correlation", *Int. J. Heat Mass Transfer* 37 (Suppl. 1), 303–309 (1994).

[29] H. Kim, J. Kim, and M. Kim, "Experimental study on CHF characteristics of water–TiO_2 nano fluids", *Nucl. Eng. Technol.* 38(1), 61–69 (2006).

[30] Y.H. Jeong, W.J. Chang, and S.H. Chang, "Wettability of heated surfaces under pool boiling using surfactant solutions and nano-fluids", *Int. J. Heat. Mass Transf.* 51, 3025–3031 (2008).

[31] R. Kamatchi, "Experimental investigations on nucleate boiling heat transfer of aqua based reduced graphene oxide nanofluids", *Int. J. Heat. Mass Transf*. 54(2), 437–451 (2018). DOI 10.1007/s00231–017–2135-z (2017)

[32] G. Harish, V. Emlin, and V. Sajith, "Effect of surface particle interactions during pool boiling of nanofluids", *Int. J. Therm. Sci.* 50, 2318–2327 (2011).